



Article

Steel-Reinforced Polymers and Steel-Reinforced Composite Mortars for Structural Applications—An Overview

Rafał Krzywoń

Faculty of Civil Engineering, Silesian University of Technology, 44-100 Gliwice, Poland; rafal.krzywon@polsl.pl; Tel.: +48-32-237-22-63

Received: 23 August 2020; Accepted: 17 September 2020; Published: 20 September 2020



Abstract: Bonding of external reinforcement is currently the simplest, fastest, and most popular method of strengthening concrete and masonry structures. Glass and carbon organic fibers are the dominant materials used, but alternatives also include high-strength steel wires. The mechanical properties of such steel are comparable to those of carbon fiber. Due to their good compatibility with mortars, steel wires are particularly well suited to the revitalization of historic buildings. The manuscript provides an overview of research and experience in the use of steel-reinforced polymers (SRPs) and steel-reinforced composite mortars (SRCMs, also called steel-reinforced grout (SRG)) for structural strengthening. The examples described are for concrete beams, slabs and columns, walls, and masonry arches. The results of laboratory tests are discussed. The summary presents the advantages and disadvantages of composites based on ultra-high-strength steels compared with more popular carbon fiber composites.

Keywords: steel-reinforced polymers (SRP) composites; steel-reinforced grout (SRG)-reinforced mortars; strengthening of structures; externally bonded reinforcement

1. Introduction

Steel-reinforced polymers (SRPs) were introduced to structural engineering applications in 2004 as an alternative to externally bonded organic-fiber-reinforced polymers. The growing market of adhesively bonded strengthening systems for reinforced concrete has spurred the development of alternatives to the dominant carbon and glass fibers. The solution was found in ultra-high-tensile-strength (UHTS) steel originally developed for the tire industry. Steel fibers with a diameter of 0.2–0.48 mm are twisted around each other to form cords or ropes. The most popular is the 3×2 cord, which is made of three straight fibers, with another two twisted around them (Figure 1). The wires are protected against rusting by brass or zinc coating. Twisting wires is an extension of the idea used, among others, in prestressing tendons; it improves adhesion to the matrix surrounding the cord. The fibers are joined crosswise to form textile tapes ready for application. Like other FRPs (fiber-reinforced polymers), tapes can be bonded by using epoxy or polyester resin, obtaining steel-reinforced polymer. Alternatively, a cement-based mortar can be used. It may lead to lower bond strength but provides better integrity with a substrate surface (e.g., in historic structures).

Outstanding strength properties make SRP composites comparable to carbon-fiber-based strengthening systems. This manuscript aims to review the current research on SRP as a material for reinforcing concrete, masonry, and timber structures. The advantages and disadvantages of SRP composites will be discussed in comparison with competing materials.

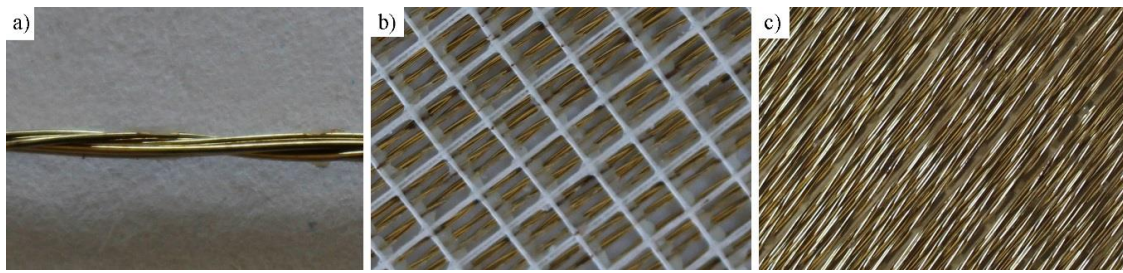


Figure 1. View of steel cord (a), low- (b), and high-density (c) ultra-high-tensile-strength (UHTS) steel textiles.

2. Properties of Steel Textiles

UHTS steels are usually made of pearlite steel. It consists of lamellar ferrite and cementite, the structure of which is strengthened in the process of patenting and drawing. The hardening effectiveness of eutectoid pearlite steel is greater than that of low-carbon ferrite single- or dual-phase steel comprising ferrite and martensite [1]. This means that even a small drawing strain increases the tensile strength effectively. For UHTS wires, it exceeds 60%. The steel is drawn down through successive dies until it reaches a diameter of 0.20–0.35 mm. Such a small diameter distinguishes the mentioned steel from other high-strength structural steels. The ultimate tensile strength of pearlite steel is estimated to be about 10 GPa [1]. Its further increase is limited by the deformability of cementite platelets. Additionally, too intensive drawing reduces ductility, and often the wire breaks from being drawn. A wire diameter of 0.20 mm is therefore a compromise between high strength and abundant ductility.

The tensile behavior of UHTS steel can be compared with that high-carbon steels commonly used in prestressed structures. It is linear elastic up to 60–70% of the ultimate strength, and then there is a gradual decrease in stiffness until the ultimate stress is attained (Figure 2). Current tests carried out on most popular 3×2 single cords either dry strips of textile [2–7] or show strength ranging from 2440 to 3302 MPa, an ultimate strain ranging from 1.6% to 2.2%, and Young's modulus ranging from 183 to 206 GPa. For less popular 3SX and 12x cord types, the strength parameters are slightly better: strength reaches 3311 MPa [4], and Young's modulus 216 GPa [3]. This phenomenon could be explained by the effect of guiding the wires. In the 3×2 cord, the two twisted wires improve the bond but are less effective in transferring tension.

The mechanical properties of ready laminate are the average properties of the fibers and the matrix. For high-density steel tape, the manufacturer recommends that the volumetric steel wire to resin ratio should be 1:1.7 [8]. Ideal application conditions are difficult to maintain, which is why most researchers of impregnated tapes give values reduced to the steel cross section. Ultimate values are measured for the cracked stage, which means that the mechanical properties are mainly governed by the properties of steel and do not differ from those specified for naked wires [5,9,10]. The values of properties based on the final cross section of the laminate are significantly lower. Depending on the type of cord, the strength varies from 950 to 1200 MPa, and the modulus of elasticity from 62.7 to 80.2 GPa [8,11]. Some stiffening effect caused by epoxy matrix can be observed in the test for laminated textiles, for the precracking stage. It is most evident for low-density tape, because the uncracked epoxy resin contributes to the stiffness. After cracking, the stiffness corresponds to that of the dry textile.

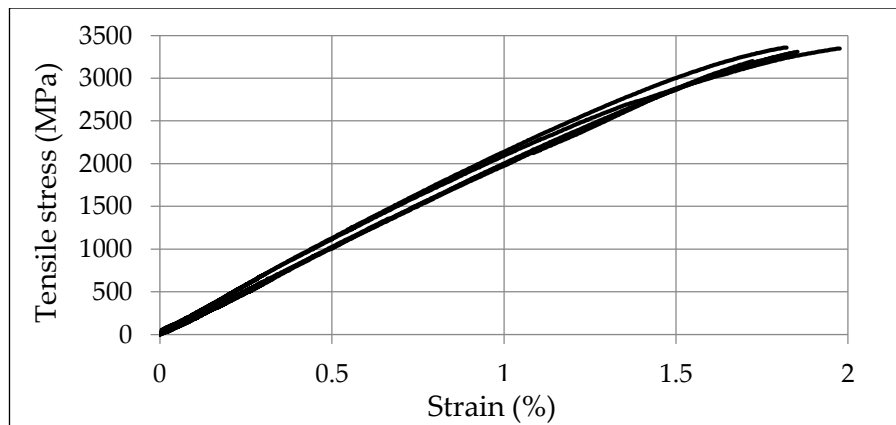


Figure 2. The stress–strain relationship for 3X2-20 steel textile.

The extremely small diameter of wires makes durability one of the most important issues for strengthening effectiveness with the UHTS steel. De Santis and de Felice [12] tested steel textiles protected by corrosion coatings and aged in substitute ocean water (according to ASTM D1141-98). Research proved that zinc coating effectively prevents rusting. After 1000 h of aging, straight cord displayed a strength reduction of about 5%, while local flexing produced a strength deterioration of 15%. More disturbing conclusions can be drawn from Borri’s team research [13]. They tested the impact of acid solution on the strength (according to ASTM G 36 standard). After 400 days, they noticed 4%, 10%, and 17% strength decreases, respectively, for specimens with any mortar applied, with a fiber-reinforced mortar, and with hydraulic mortar covering. An even greater drop of strength applies to samples naturally aged in outdoor conditions. In the cited studies, it reached 20% and 44%, respectively, for uncast specimen and specimen cast in hydraulic mortar. Additionally, the degradation of the interface between the fiber and the matrix was observed in both moisture and alkaline environments.

3. Bond Behavior

For externally bonded fiber-reinforced polymers, the bond strength determines the effectiveness of strengthening. In most cases, failure occurs due to detachment of the composite overlay before its tensile strength is attained. Among the test procedures, the most popular are the single-lap direct shear test and the double-lap direct shear tests. Among the more unique ones can be found the notched beam test.

Many bond test results can be found in the literature. Some of them were made to standardize the procedures for determining bond, others for further tests or numerical analyses. Some of them concern specially prepared elements for test purposes, others extracted from the existing structure (reinforced concrete bridge, masonry).

Among the factors influencing the bond, the following are important:

- composite properties (modulus of elasticity, anchorage length, width, thickness),
- substrate properties (compressive strength, tensile strength, surface condition),
- type of adhesive (epoxy, mortar, flexible polyurethane),
- environmental conditions (temperature, humidity),
- application conditions (relation to the element size, method of covering).

Figures 3 and 4 show the results of selected bond strength tests. As usual, the weakest element of the system is the strength of the substrate [14]; it has been referred to in this feature. There is a large variability in the results. Relating them to the strength of UHTS steel, the exploitation ratio ranges between 13% and 92% for concrete substrate and from 17% to 95% for masonry. Even in research by the same author, there are big differences. Their main reason is the variation in anchorage length.

For concrete, the effective transfer length is estimated to be between 127 and 150 mm. For brick substrate, due to its lower strength, it is a little longer and recommended to be between 170 and 190 mm.

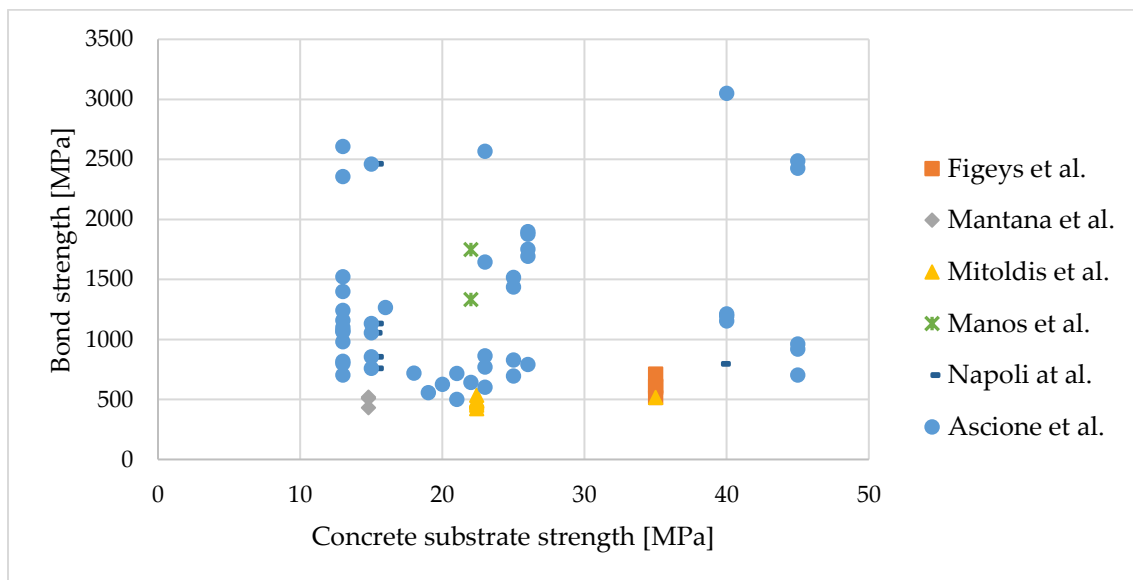


Figure 3. Review of bond strength test results concerning concrete substrate [15–20].

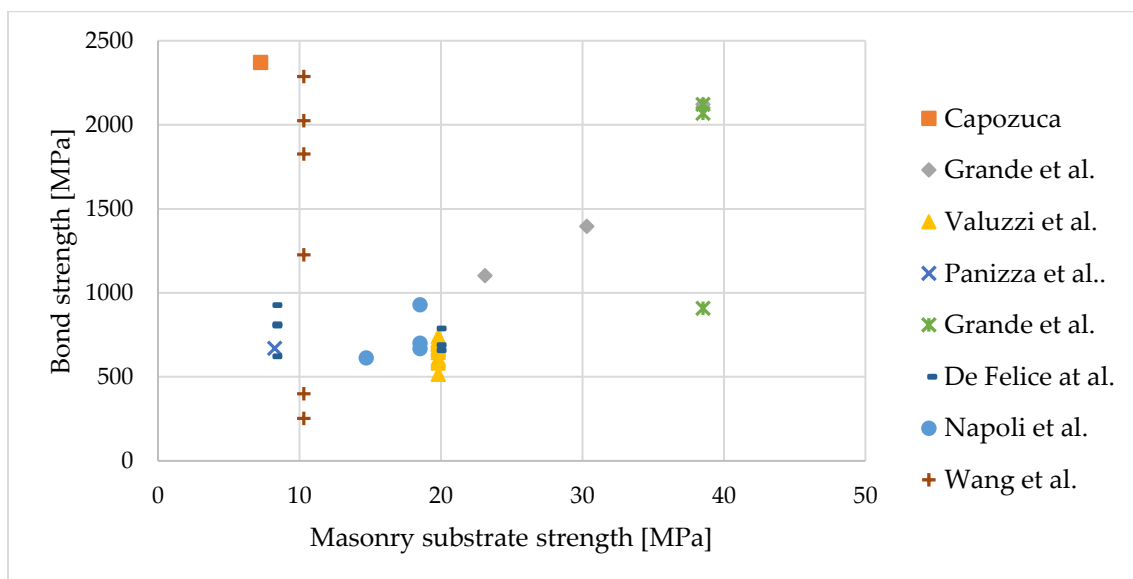


Figure 4. Review of bond strength test results concerning masonry substrate [7,9,19,21–25].

As can be expected, the bonding performance of high-density textile is lower compared with that of low-density textile. The reason is a smaller area through which the adhesive force is transmitted for a single cord. Another issue is the ability to penetrate the resin or mortar through the densely packed cord [26]. Due to bond limits, in some cases it may not be advantageous to use high-density steel fabrics [14]. Also, application of a second layer of steel tape does not proportionally increase the bearing capacity of the strengthening system.

The role of adhesive density was investigated by Grande et al. [24]. They found that low-density adhesives penetrate the masonry substrate and showed a decohesion failure mechanism, which involves the material composing the support. In medium-density epoxy adhesive and grout, failure occurs in the layer of adhesive. This phenomenon was also confirmed by Ascione [26] and Bencardino [27]. Irrespective of the surface finish and the steel fiber density, the dominant failure mode

for concrete is cohesive debonding within the concrete substrate [20]. The ultimate bond of systems based on epoxies is generally two to three times greater than that based on the mortar matrix [16,28]. According to Wang et al. [25], steel textile with a cement-based mortar matrix has a higher bond stiffness and bond strength, but lower ultimate slip than that with a lime-based mortar matrix. The research of De Santis et al. [29] shows that the worst bond provides the lime- and pozzolan-based mortar; the bond properties of the geopolymer and lime-based mortar are comparable.

In the case of a cement matrix, three forms of debonding failure are possible: debonding at the matrix–masonry interface, interlaminar failure at the matrix–fiber interface, and rupture of the steel wires. The most common is interlaminar failure [30]. According to Razavizadeh et al. [31], the surface preparation is the first factor determining the failure mode. A strong brick–mortar interface determines the failure at the steel–mortar interface. Santis et al. [29] indicate the mechanical properties of the matrix, cord surface smoothness, the curing and manufacturing conditions as among the other important factors. Especially the last phenomenon was evidenced by the cited round robin test.

Elmahdy et al. [32] proved that sandblasting increases adhesion to UHPC (ultra-high-performance concrete) more than 2.5 times. According to Ascione et al. [14], bush hammering increases the ultimate bond capacity more effectively than grinding or sandblasting. Surface preparation is less important in systems based on a weaker mortar matrix [16]. Application on weaker surfaces, such as old brick, even with good adherence, does not guarantee an adequate bond strength due to the danger of detachment with a thin layer of support material [22].

Mechanical anchorage may be a remedy for insufficient adhesion. The methods used include transverse overlapping, chemical anchors, through element bolts, and anchored transverse steel sections. The last listed anchoring device can increase the ultimate capacity four times [18].

From a practical point of view, bond durability is important. Al Khafaji et al. [33] tested samples conditioned in the chamber and real-time weather. Regardless of the type of cord protection (galvanizing and brass coating), the ultimate bond reduced significantly, in the worst case, up to 22% after 1 year of conditioning. A little more optimistic conclusion comes from Gentilini's research [34]. Conditioned in saline solution, specimens did not exhibit a significant decrease in bond capacity; however, there was salt accumulation observed in the material pores. The best protection offers a nonporous highly deformable polyurethane matrix. De Santis et al. [35] proved that artificial weathering in high humidity and drying cycles did not produce any noticeable deterioration of the bond. Only immersion in substitute ocean water solution caused corrosion of locally uncovered steel wires, but without bond strength reduction or modification of the failure mode. It should be noted here that highly deformable polyurethane is relatively new material, and in SRP applications, it still requires better understanding. Research provided by Kwiecien et al. [36] proved that in clay, brick substrate polyurethane matrix increases the ultimate bond by 80%.

Thermal conditioning also does not favorably affect mortar-based steel textile composites. Based on Ombres's research [37], temperatures below 100 °C can be considered safe for steel-reinforced cementitious matrix. At a temperature of 150 °C, the strength drops by 30%. The destruction itself is certainly fragile, and the global slip at 200 °C is over six times lower.

4. Application on Concrete Substrates

4.1. Bending Strengthening of Beams and Slabs

Beam strengthening can be considered the first application area of UHTS steel textile composites. The first studies often concerned the repair of existing structures, mainly bridges [2,38,39] and floor beams [40].

As reported by the researchers, the strengthening efficiency of steel textile composites is from 18% [8] to over 300% [41]. Of course, that efficiency only partly depends on the composite strength. It is also a result of the beam material properties, geometry, and intensity of the reinforcement. For these reasons, this chapter does not present a comparison of the tests but shows the properties

of steel textile composites compared with other composites and the specificity of the behavior of the strengthened beams.

When compared with CFRP (carbon fiber reinforced polymer) strips, the effectiveness of SRP strengthening is reported to be similar [42]; however, usually the tensile strength of the steel cord is exploited more than that of the carbon laminate [43]. This phenomenon shows that a lower amount of SRP can be used to gain a similar strengthening effect. Steel textiles highlight their advantages when bonded with mortars. In Escrig's research [44], steel composite was the best-performing composite in terms of increasing the flexural capacity. It was also the only strengthening that offered an increasing flexural stiffness during all the stages of loading.

Balsamo [43] reported no significant difference between using epoxy adhesive and using cement-based mortar for bonding steel fabrics. Similar conclusions come from Napoli's research [6]. This phenomenon was not confirmed by Bencardino [45], who reported twice the effectiveness of the epoxy adhesive. The highest SRP efficiency was also achieved by Prota [46] and Huang [47].

The most typical failure mode is intermediate debonding [48] (Figure 5). End anchoring using U-wraps provides end debonding with rupture of the wrapping wires [45]. Another possible failure process begins with the formation of a critical diagonal crack. That crack initiates debonding, which propagates with concrete cover spalling until the midspan section. A consequence of cover delamination failure is lower ductility in the postpeak phase [49]. In the case of specimens strengthened with low-density tape, there is possible failure due to fracture of the sheet [6].

Increasing the number of strengthening composite layers does not increase the flexural capacity correspondingly. Alghazali and Myers [50] showed that an additional layer of mid-density SRP increases the load capacity by only 10%. In too extensive strengthening premature debonding, failure occurs. On the other hand, stronger reinforcement (e.g., using a denser tape) increases the stiffness of the beam [49].

The presence of strengthening has a slight influence on the cracking moment and the crack spacing. In general, the crack spacing depends on the position of the stirrups. In Ceroni and Pecce's research [3], a slightly smaller crack spacing occurred only at failure conditions. The beams externally reinforced were characterized by a more irregular crack pattern due to local debonding at the concrete–laminate interface. Kim et al. [51] showed that crack spacing could be reduced by U-wrapping. Pecce's tests [52] have shown that the crack spacing decreases when a wider laminate is used.



Figure 5. Debonding failure of beam strengthened with two layers of SRP textile composite.

Alghazali et al. [53] tested extremely damaged RC (reinforced concrete) beams repaired and strengthened with SRP overlays. They reported that the original capacity can be restored when strengthening consists of two SRP layers with five U-wraps. U-wrapping improved the failure mode. Only local debonding in the SRP system was observed. Steel fabric may be integrated with a concrete repair system. Such a solution based on reprofiling geopolymer mortar was tested by

Bencardino and Condello [54,55] and was found to be more effective than the traditional epoxy-based bonding technique.

Durability tests provided by Al-Nuaimi et al. [56] have proven the resistance of epoxy-based steel textile to sun and saline water. A 24-month exposure showed only a marginal loss of strength.

SRP strengthening improves fatigue resistance. A test provided by Katatklos et al. [57] showed an increase in stiffness and thus a reduction in steel stress. Used in the cited research, organic matrix proved fatigue resistance. All the beams failed primarily due to fatigue of the steel reinforcement. Fiber debonding was a secondary failure mechanism. Minnaugh [58] reported better fatigue behavior of SRP tapes compared with CFRP.

4.2. Shear Strengthening of Beams

FRP shear strengthening is based on the assumption that external jacketing plays a role similar to that of stirrups in carrying diagonal tensile stresses. It can be applied as a continuous covering of the whole length of the specimen or uniaxial tapes bonded at some intervals. The short height of the side surface of beams implicates the correct anchoring of the reinforcement. The easiest solution is to fully wrap the beam, but in practice, due to the connection with the ceiling structure, it is usually not possible. Therefore, U-wraps associated with mechanical anchorage are usually used. The effectiveness of mechanical anchoring has been confirmed by the studies of Mitoldis [59], Papakonstantinou [60], Vakjira [61], and Thermou [62]. Only Gonzales [63] did not report a significant increase in shear strength.

The failure mode depends on the intensity of strengthening. A fully wrapped strong reinforcement moves the failure into the flexure zone [62]. A single-layered and fully wrapped beam fails due to the presence of a shear–flexure crack. The U-wrapped SRG beam fails in shear due to the detachment of the composite. The use of mechanical anchors allows for better utilization of strengthening material [60]. The presence of anchors helps to avoid premature debonding [63]. The ductility of the beams in case of a wrapped or anchored system is also greater, avoiding brittle failure.

The fiber exploitation ratio depends on the axial stiffness of strengthening; therefore, the use of high-modulus carbon fibers guarantees better results than the use of steel composite [63].

Internal–external shear reinforcement interaction could be observed; thus the effectiveness of composite strengthening is related to the spacing of the internal reinforcement. According to Gonzales [63], a larger increase in shear stress may be observed for larger stirrup spacing.

4.3. Confinement of Columns

Strengthening of reinforced concrete columns by wrapping them with flexible FRP sheets is one of the most popular techniques nowadays. It efficiently enhances the strength and ductility of the concrete; however, among other advantages, there are also the low weight, minimum change in geometry, and rapid installation [64].

As a result of confinement, triaxial compression occurs in the concrete (Figure 6). Only the circular cross section of the column allows for an even distribution of stresses. In square or rectangular column strengthening, the effect is significantly lower [65]. The axial capacity can be simply improved by the rounding of the corners. The capacity and ductility increase with an increasing corner radius. El-Hacha [65] specified the minimum radius of such rounding to be 2.5 cm. For $2r/b = 0.67$ (where r is the radius, and b is the side dimension), Thermou [66] reported a confinement effectiveness that was comparable to that of a circular column. She also pointed out the advantages of using mortar matrices resulting from the stress smearing action at the corners. The rounding effect was not confirmed by Carloni [67]. For specimens with sharp corners, he achieved higher values of the load than those of specimens with rounded corners. Because of that specific behavior, he reported the effect of delay on the opening of the SRP jacket in sharp edges. This indicates the importance of proper anchoring of the confinement. According to Thermou and Hajirasouliha [68], in the SRG jacket, the use of a 360 mm overlap ensures the rupture of the low- and medium-density fabric [69]. The use of a higher-density

fabric or two-layered systems leads to debonding or a mixed failure mode. The bond may be improved by concrete surface treatment (e.g., sandblasting) [70].

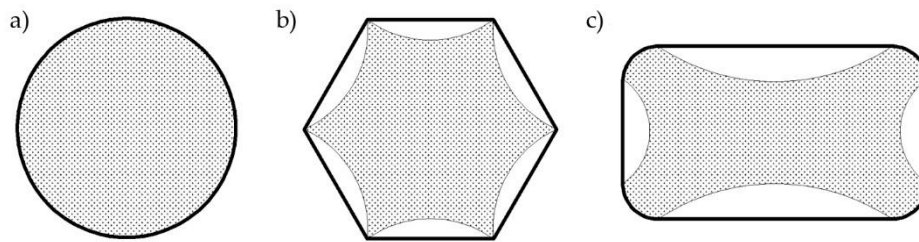


Figure 6. Effect of shape on confinement effectiveness: (a) circular section, (b) hexagonal section, (c) rectangular section with rounded corners.

Wrapping reduces the lateral deformation of columns but does not prevent the typical failure due to the buckling of the main rebars [71].

Increasing the number of strengthening layers directly enhances the confinement pressure. According to Thermou's [68] research, one-layered low-density SRG jackets can increase the strength capacity of unconfined specimens by up to 40%, while two-layered high-density confinement increases the load capacity by 193%. Even better effectiveness, but for polymer-based SRP confinement, was reported by Napoli and Realfonzo [72]. Double wrapping allowed the increase of concrete compressive strength over 13 times. Strength increase does not have a linear relationship with the number of SRP layers [73]. Confinement effectiveness also decreases in concrete with higher strength [74]. It should be emphasized that Napoli's results were obtained for relatively low and axially loaded specimens. According to El-Hacha and Abdelrahman's [73] research, increasing slenderness reduces the percentage increases in ultimate axial strength, axial and hoop strains, and strain efficiency of SFRP wrapped specimens. A triple increase in slenderness reduces confinement pressure by 30%. In compression with associated bending, SRP confinement does not increase the flexural strength; however, it allows the achievement of a significantly higher ductility [75]. Flexural capacity can be improved by the addition of longitudinal SRP sheets [76]. In dynamic influences (e.g., earthquake), a fast-rate load may reduce confinement effectiveness [77].

Abdelrahman [78] reported higher strain efficiency in SRP wrapping compared with that in CFRP confinement. SRP sheets provided a higher percentage contribution toward the total ductility of the columns than CFRP sheets.

4.4. Retrofitting of Beam–Column Joints

The main motivation for conducting research on the strengthening of beam–column joints is their frequent damage caused by earthquakes (Figure 7). These zones are often characterized by the absence of stirrups, non-optimal arrangement of transverse and/or longitudinal rebars, or manufacturing with low-quality concrete [79].

Thermou et al. [80] tested damaged reinforced concrete columns and then retrofitted them with metallic fabric jackets made of SRG. The retrofitted specimens increased both their strength and deformation capacity. One layer of the metallic fabric jacket exhibited excellent behavior compared with three layers of glass- and carbon-FRP jackets.

Vita et al. [79] tested 3D reinforced concrete joints strengthened with medium-density SRP tape. They considered two types of strengthening layouts: “cross,” where a steel cord was applied orthogonally in the directions of the beams and column, and “diagonal,” where strengthening diagonally wrapped the joint. All the SRP-strengthened specimens failed due to a large flexural crack at the column–main beam interface, followed by damage to the joint panel and delamination of the SRP tapes. The SRP-strengthened specimens exhibited a load capacity increase over the control member not greater than 17%, and ductility increased in the range 10–28%.



Figure 7. SRP strengthened the frame of a multistory building.

5. Applications on Brickwork Substrates

5.1. Strengthening of Arches

The application of composite strengthening at the intrados or extrados of vaults alters the mechanism of the formation of plastic hinges. A detailed description of the failure mechanism can be found in [81]. In general, fibers can bear the stresses occurring at the tensed edges and thus prevent the formation of a fourth joint, which usually leads to the arch collapsing.

Borri et al. [82] tested the behavior of strengthened arches under a monotonic vertical load applied at a quarter of their span. Reinforcement was applied to extrados, intrados, and both surfaces. The received increases provided by the steel cords were greater than those obtained using carbon fibers. In the intrados strengthening, the SRG was more effective in engaging the masonry substrate. Additionally, a significant role of mechanical anchoring was observed and allowed for the increase of load capacity by 72%. The highest bearing capacity had the specimen that was reinforced on both sides (intrados and extrados). The reinforcement site also determined the model of destruction. Externally strengthened arches failed due to shear sliding of the masonry, while internal strengthening failed due to laminate rupture or debonding. Similar conclusions can be found in Girardello's research [83]. He conducted tests under cyclic load masonry arches strengthened in the extrados. To prevent anchorage sliding, he proposed steel spikes near the support. The highest load capacity was obtained for the SRP-strengthened arch. It failed due to crushing. Because of the tape's density, the efficiency of the reinforcement with the SRG composite was considered to be better. Its ductility was also unrivaled.

Better ductility may be caused by the greater density of steel textile. Garmendia's comparative research [84] shows very similar deformability of SRG- and SRP-strengthened arches. The same UHTS steel tape was used in these tests. Despite these similarities, the failure pattern of the sample reinforced with the SRP tape was different. The SRG postponed the hinge formation, while the SRP solution prevented its formation, and the arch failed due to sliding between voussoirs near the keystone.

Carozzi [85] tested in situ ribbed barrel vaults belonging to an ancient masonry building. The lime-based mortar SRG system increased the load capacity four times. This result was comparable to that for CFRP but slightly lower than that for glass-fiber-based TRM (textile-reinforced mortar). The application of SRG caused a relevant increment in the stiffness of the structure. At the postpeak phase, strengthening was able to carry a fairly constant load until collapse.

5.2. Reinforcing of Walls

Strengthening walls may include in-plane and out-of-plane failure cases. A composite material can be very helpful in preventing the out-of-plane brittle collapse of slender infill walls in modern buildings. Valluzzi et al. [86] tested masonry panels subjected to four-point bending tests. The panels were strengthened unidirectionally with various types of composites. The best-performing materials in terms of bearing capacity were indicated to be CFRP and high-density SRP. Among composites based

on a friendlier inorganic matrix, the best ones turned out to be low-density SRG and basalt-based TRM. The best behavior of SRG was achieved when magnesia mortar was used as a matrix. For SRGs, failure due to matrix slipping and slippage of fibers was characteristic, while for SRP, shear debonding was observed.

Out-of-plane tests were also conducted by Parsekian [87]. The investigations included orthogonally strengthened samples tested in the direction of the vertical and horizontal span. The research confirmed the effectiveness of SRP strengthening, although results were slightly lower than those for sprayed glass-fiber-reinforced polymer. An interesting fact is that the increase in strength of the vertical span specimens was much higher than that in horizontal cases.

The in-plane behavior of SRG-strengthened masonry panels was studied by Borri [88]. The results indicated a significant shear strength increase for both types of steel cords used. The most effective results were achieved for low-shear strength masonry, based on hydraulic lime mortar. Double-side strengthening provided greater strength increases than single-side strengthening. Additionally, the strip width effect was observed. The greatest increase in load capacity occurred in the specimens strengthened with 50 mm wide SRG strips.

5.3. Confinement of Masonry Columns

As in reinforced concrete structures, the strengthening of masonry columns is aimed at increasing the load-bearing capacity by introducing a triaxial state of stress. Masonry columns are often elements of historic buildings, where maintaining dimensions and shapes are the main conditions for repair. SRP overwrapping of the column allows for meeting this requirement.

Borri et al. [89] tested rectangular, square, and octagonal columns wrapped with continuous and discontinuous SRP sheets. They proved that confinement significantly improves both the load-carrying capacity and deformability; however, lower effectiveness was obtained from rectangular columns. This was caused by the lower effective area of the confined cross section in the rectangular columns. Two types of cord were used in the cited research. Better efficiency was noted in the 3X2 cord type. The failure mode was very similar, regardless of the shape and method of wrapping [4]. Progressive transversal dilation with the growth of vertical cracks through mortar joints was terminated by the failure of the confinement. Wrapping failure occurred midway up the column and involved approximately one-third of the column height.

Sneed et al. [90–92] tested short brick masonry columns with a square cross section confined by SRG jackets under a monotonic concentric compressive load. The results showed that SRG jacketing increased the load capacity by 26–41% relative to unconfined column. The effectiveness of the strengthening depended on the density of the fibers, but its increase was not proportional. There were also a slight effect of mortar grade and a favorable effect of corner radius ratio.

The density of the fiber and corner rounding affect ductility. Generally, the higher is the wire density, the greater is the axial strain at the peak stress. The exception is a sharp corner where the strain may increase with a decrease of fiber density [93].

Ombres and Verre [94] tested square columns confined with a steel-FRCM (fibre reinforced composite mortar) strengthening. They used inorganic mortar matrix-based lime and a mineral binder (intended for highly breathable historical masonry restoration). The tests confirmed the effectiveness of strengthening in increasing the bearing capacity. Also, the ductility of axially loaded columns increased with the confinement ratio. Only in eccentrically loaded columns did the ductility index turn out to be less favorable.

An interesting solution was proposed by Fossetti and Minafo [95]. They introduced four high-strength steel wires as a wrapping in the horizontal mortar joints. Wires were tightened by hand-pinch closing, and joints were filled with fiber-reinforced mortar. The technique proved effective with weak mortars; however, its weak point was a failure due to the opening of the wires' knots.

6. Strengthening of Timber

The application of composites seems ideal for a wooden structure. Technically, wood is a natural polymer matrix composite material reinforced with continuous cellulose fibers. High-strength fiber can locally improve mechanical properties. The bibliography on the use of fiber composites for timber strengthening is very broad, but it concerns the use of organic fibers. Against this background, there are very few studies on UHTS steel-based composites.

Borri and Corradi [96] tested timber beams strengthened along the tensile zone with two types of SRP tape. The investigations were preceded by bonding tests. They showed that bond strength is extremely sensitive to anchorage length. The most effective bond length was identified to be 100 mm, beyond which no strength enhancement occurred. Application of flexural strengthening enhanced the flexural capacity and ductility of beams. In some cases, the strengthening effect exceeded 100% in the ultimate load compared with the unstrengthened beam. Failure occurred as a result of strengthening detachment or wood tension failure preceded by a high level of wood yielding in compression.

Dager and Sanchez [97] tested glulam beams strengthened by bonding an additional layer containing SRP reinforcement. They achieved a 26% increase in load capacity. The doubling of the SRP composite layer allowed for the increase of the load-bearing capacity by 37%, and at the same time, damage occurred due to wood compression.

7. Conclusions

The research results presented in the manuscript show the great potential of steel textile composites, especially in areas where it is necessary to adjust the shape. Thanks to their much greater flexibility compared with pultruded carbon fibers, they allow for strengthening by wrapping columns, beams, and even frame joints. The effectiveness of such reinforcements is at the level of carbon fibers and far exceeds the potential of other types of organic fibers.

Another advantage of steel textiles is their excellent compatibility with grout matrices. This opens up new application areas, especially in historic buildings, where water vapor permeability and easy removability are required. The application of mortar adhesives is easier; they can be used on a humid substrate. The emission of toxic substances is incomparably smaller. Grout adhesives also perform better at elevated temperatures.

The manuscript omits the theoretical part of research on steel textile composites, numerical models, and analytical models that can be used in the design. Similarities to other types of composites mean that nowadays steel textiles are designed and used according to standards and guidelines developed mainly for strengthening with the use of carbon fibers. Only durability, especially corrosion resistance, should be given additional attention.

Funding: This research was funded by Silesian University of Technology, grant BK-237/RB6/2020.

Conflicts of Interest: The author declares no conflict of interest.

References

1. Tashiro, H. The Challenge for Maximum Tensile Strength Steel Cord. *Nippon Steel Tech. Rep.* **1999**, *80*, 6–8.
2. Lopez, A.; Galati, N.; Alkhrdaji, T.; Nanni, A. Strengthening of a reinforced concrete bridge with externally bonded steel reinforced polymer (SRP). *Compos. Part B Eng.* **2007**, *38*, 429–436. [[CrossRef](#)]
3. Ceroni, F.; Pecce, M. Cracking behaviour of RC beams externally strengthened with emerging materials. *Constr. Build. Mater.* **2007**, *21*, 736–745. [[CrossRef](#)]
4. Borri, A.; Castori, G.; Corradi, M. Masonry Columns Confined by Steel Fiber Composite Wraps. *Materials* **2011**, *4*, 311–326. [[CrossRef](#)]
5. De Santis, S.; de Felice, G. Tensile behaviour of mortar-based composites for externally bonded reinforcement systems. *Compos. Part B* **2015**, *68*, 401–413. [[CrossRef](#)]
6. Napoli, A.; Realfonzo, R. Reinforced concrete beams strengthened with SRP/SRG systems: Experimental investigation. *Constr. Build. Mater.* **2015**, *93*, 654–677. [[CrossRef](#)]

7. De Felice, G.; Aiello, M.A.; Bellini, A.; Ceroni, F.; De Santis, S.; Garbin, E.; Leone, M.; Lignola, G.P.; Malena, M.; Mazzotti, C.; et al. Experimental characterization of composite-to-brick masonry shear bond. *Mater. Struct.* **2016**, *49*, 2581–2596. [[CrossRef](#)]
8. Kim, Y.J.; Fam, A.; Kong, A.; El-Hacha, R. Flexural strengthening of RC beams using steel reinforced polymer (SRP) composites. *ACI Spec. Publ.* **2005**, *230*, 1647–1664.
9. Panizza, M.; Garbin, E.; Valluzzi, M.R.; Modena, C. Experimental investigation on bond of FRP/SRP applied to masonry prisms. In Proceedings of the Conference CICE, Rome, Italy, 13–15 June 2012.
10. Krzywon, R. Features of SRP Tapes against CFRP Composites Used for Strengthening of Concrete Structures. *Procedia Eng.* **2017**, *193*, 289–296. [[CrossRef](#)]
11. Mitolidis, G.J.; Salonikios, T.N.; Kappos, A.J. Mechanical and Bond Characteristics of SRP and CFRP Reinforcement—A Comparative Research. *Open Constr. Build. Technol. J.* **2008**, *2*, 207–216. [[CrossRef](#)]
12. De Santis, S.; de Felice, G. Steel reinforced grout systems for the strengthening of masonry structures. *Compos. Struct.* **2015**, *134*, 533–548. [[CrossRef](#)]
13. Borri, A.; Castori, G.; Corradi, M.; Speranzini, E. Durability Analysis for FRP and SRG Composites in Civil Applications. *Key Eng. Mater.* **2015**, *624*, 421–428. [[CrossRef](#)]
14. Ascione, F.; Lamberti, M.; Napoli, A.; Razaqpur, G.; Realfonzo, R. An experimental investigation on the bond behavior of steel reinforced polymers on concrete substrate. *Compos. Struct.* **2017**, *181*, 58–72. [[CrossRef](#)]
15. Figeys, W.; Schueremans, L.; Van Gemert, D.; Brosens, K. A new composite for external reinforcement: Steel cord reinforced polymer. *Constr. Build. Mater.* **2008**, *22*, 1929–1938. [[CrossRef](#)]
16. Matana, M.; Nanni, A.; Dharani, L.; Silva, P.; Tunis, G. Bond Performance of Steel Reinforced Polymer and Steel Reinforced Grout. In Proceedings of the International Symposium on Bond Behaviour of FRP in Structures (BBFS 2005), IFRPC, Hong Kong, China, 7–9 December 2005.
17. Mitolidis, G.I.; Kappos, A.J.; Salonikios, T.N. Bond tests of SRP and CFRP—strengthened concrete prisms. In Proceedings of the Fourth International Conference on FRP Composites in Civil Engineering (CICE2008), Zurich, Switzerland, 22–24 July 2008.
18. Manos, G.C.; Katakalos, K.; Kourtidis, V. The influence of concrete surface preparation when fiber reinforced polymers with different anchoring devices are being applied for strengthening R/C structural members. *Appl. Mech. Mater.* **2011**, *82*, 600–605. [[CrossRef](#)]
19. Napoli, A.; de Felice, G.; De Santis, S.; Realfonzo, R. Bond behaviour of Steel Reinforced Polymer strengthening systems. *Compos. Struct.* **2016**, *152*, 499–515. [[CrossRef](#)]
20. Ascione, F.; Napoli, A.; Realfonzo, R. Experimental and analytical investigation on the bond of SRP systems to concrete. *Compos. Struct.* **2020**, *242*, 112090. [[CrossRef](#)]
21. Capozucca, R. Experimental FRP/SRP—historic masonry delamination. *Compos. Struct.* **2010**, *92*, 891–903. [[CrossRef](#)]
22. Grande, E.; Imbimbo, M.; Sacco, E. Bond Behavior of Historical Clay Bricks Strengthened with Steel Reinforced Polymers (SRP). *Materials* **2011**, *4*, 585–600. [[CrossRef](#)]
23. Valluzzi, M.R.; Oliveira, D.V.; Caratelli, A.; Castori, G.; Corradi, M.; de Felice, G.; Garbin, E.; Garcia, D.; Garmendia, L.; Grande, E.; et al. Round Robin Test for composite-to-brick shear bond characterization. *Mater. Struct.* **2012**, *45*, 1761–1791. [[CrossRef](#)]
24. Grande, E.; Imbimbo, M.; Sacco, E. The role of the adhesive on the bond behavior of SRPs applied on masonry supports: Experimental and numerical study. *Key Eng. Mater.* **2015**, *624*, 652–659. [[CrossRef](#)]
25. Wang, X.; Lam, C.C.; Iu, V.P. Bond behaviour of steel-TRM composites for strengthening masonry elements: Experimental testing and numerical modelling. *Constr. Build. Mater.* **2020**, *253*, 119157. [[CrossRef](#)]
26. Ascione, F.; Lamberti, M.; Napoli, A.; Realfonzo, R. Experimental bond behavior of Steel Reinforced Grout systems for strengthening concrete elements. *Constr. Build. Mater.* **2020**, *232*, 117105. [[CrossRef](#)]
27. Bencardino, F.; Condello, A.; Ashour, A.F. Single-lap shear bond tests on Steel Reinforced Geopolymeric Matrix-concrete joints. *Compos. Part B* **2017**, *110*, 62–71. [[CrossRef](#)]
28. Grande, E.; Imbimbo, M.; Sacco, E. Investigation on the bond behavior of clay bricks reinforced with SRP and SRG strengthening systems. *Mater. Struct.* **2015**, *48*, 3755–3770. [[CrossRef](#)]
29. De Santis, S.; Ceroni, F.; de Felice, G.; Fagone, M.; Ghiassi, B.; Kwiecień, A.; Lignola, G.P.; Morganti, M.; Santandrea, M.; Valluzzi, M.R.; et al. Round Robin Test on tensile and bond behaviour of Steel Reinforced Grout systems. *Compos. Part B* **2017**, *123*, 100–120. [[CrossRef](#)]

30. Santandrea, M.; Focacci, F.; Mazzotti, C.; Ubertini, F.; Carloni, C. Determination of the interfacial cohesive material law for SRG composites bonded to a masonry substrate. *Eng. Fail. Anal.* **2020**, *111*, 104322. [[CrossRef](#)]
31. Razavizadeh, A.; Ghiassi, B.; Oliveira, D.V. Bond behavior of SRG-strengthened masonry units: Testing and numerical modeling. *Constr. Build. Mater.* **2014**, *64*, 387–397. [[CrossRef](#)]
32. Elmahdy, A.; El-Hacha, R.; Shrive, N.G. Bonding of CFRP and SRP to Ultra-high Performance Concrete. In Proceedings of the Asia-Pacific Conference on FRP in Structures (APFIS 2007), IIFRPC, Hong Kong, China, 12–14 December 2007; pp. 686–689.
33. Al-Khafaji, A.F.; Myers, J.J.; Wang, W. Bond evaluation of SRP strengthening system exposed to several harsh environmental conditions. *Constr. Build. Mater.* **2020**, *231*, 117093. [[CrossRef](#)]
34. Gentilini, C.; Franzoni, E.; Santandrea, M.; Carloni, C. Salt-Induced Deterioration on FRP-Brick Masonry Bond. In *Structural Analysis of Historical Constructions*; RILEM Bookseries 18; Aguilar, R., Torrealva, D., Moreira, S., Pando, M.A., Ramos, L.F., Eds.; Springer: Berlin/Heidelberg, Germany, 2019; pp. 1914–1921.
35. De Santis, S.; Stryzewska, T.; Bandini, S.; de Felice, G.; Hojdys, Ł.; Krajewski, P.; Kwiecień, A.; Roscini, F.; Zając, B. Durability of steel reinforced polyurethane-to-substrate bond. *Compos. Part B* **2018**, *153*, 194–204. [[CrossRef](#)]
36. Kwiecien, A.; Krajewski, P.; Hojdys, Ł.; Tekieli, M.; Słonski, M. Flexible Adhesive in Composite-to-Brick Strengthening—Experimental and Numerical Study. *Polymers* **2018**, *10*, 356. [[CrossRef](#)] [[PubMed](#)]
37. Ombres, L.; Iorfida, A.; Mazzuca, S.; Verre, S. Bond analysis of thermally conditioned FRCM-masonry joints. *Measurement* **2018**, *125*, 509–515. [[CrossRef](#)]
38. Rosenboom, O.; Walter, C.; Rizkalla, S. Strengthening of prestressed concrete girders with composites: Installation, design and inspection. *Constr. Build. Mater.* **2009**, *23*, 1495–1507. [[CrossRef](#)]
39. Cuzzilla, R.; Di Ludovico, M.; Prota, A.; Manfredi, G. Seismic Rehabilitation of RC Bridges by Using FRP and SRP: Case Study of a Bridge in the South of Italy. *ACI Spec. Publ.* **2011**, *277*, 1–20.
40. Casadei, P.; Nanni, A.; Alkhrdaji, T.; Thomas, J. Performance of Double-T Prestressed Concrete Beams Strengthened with Steel Reinforced Polymer. *Adv. Struct. Eng.* **2005**, *8*, 427–442. [[CrossRef](#)]
41. Saber, N.; Hassan, T.; Abdel Fayad, A.S.; Gith, H. Flexural behavior of concrete beams strengthened with steel reinforced polymers. In Proceedings of the Fourth International Conference on FRP Composites in Civil Engineering (CICE2008), Zurich, Switzerland, 22–24 July 2008.
42. Krzywon, R. Effectiveness of SRP Flexural Strengthening Compared To CFRP Strips. *Archit. Civ. Eng. Environ.* **2015**, *4*, 39–44.
43. Balsamo, A.; Nardone, F.; Iovinella, I.; Ceroni, F.; Pecce, M. Flexural strengthening of concrete beams with EB-FRP, SRP and SRCM: Experimental investigation. *Compos. Part B* **2013**, *46*, 91–101. [[CrossRef](#)]
44. Escrig, C.; Gil, L.; Bernat-Maso, E. Experimental Comparison of Reinforced Concrete Beams Strengthened Against Bending With Different Types of Cementitious-Matrix Composite Materials. *Constr. Build. Mater.* **2017**, *137*, 317–329. [[CrossRef](#)]
45. Bencardino, F.; Condello, A. Structural behaviour of RC beams externally strengthened in flexure with SRG and SRP systems. *Int. J. Struct. Eng.* **2014**, *5*, 346–368. [[CrossRef](#)]
46. Prota, A.; Tan, K.Y.; Nanni, A.; Pecce, M.; Manfredi, G. Performance of Shallow Reinforced Concrete Beams with Externally Bonded Steel-Reinforced Polymer. *ACI Struct. J.* **2006**, *103*, 163–170.
47. Huang, X.; Birman, V.; Nanni, A.; Tunis, G. Properties and potential for application of steel reinforced polymer and steel reinforced grout composites. *Compos. Part B* **2005**, *36*, 73–82. [[CrossRef](#)]
48. Bencardino, F.; Carloni, C.; Condello, A.; Foacci, F.; Napoli, A.; Realfonzo, R. Flexural behaviour of RC members strengthened with FRCM: State-of-the-art and predictive formulas. *Compos. Part B* **2018**, *148*, 132–148. [[CrossRef](#)]
49. Hawileh, R.A.; Nawaz, W.; Abdalla, J.A. Flexural behavior of reinforced concrete beams externally strengthened with Hardwire Steel-Fiber sheets. *Constr. Build. Mater.* **2018**, *172*, 562–573. [[CrossRef](#)]
50. Alghazali, H.H.; Myers, J.J. Flexural Performance of RC One-Way Slabs Strengthened with Composite Materials. *J. Mater. Civ. Eng.* **2018**, *30*, 04018120.
51. Kim, Y.J.; Fam, A.; Green, M.F. Application of SRP Composite Sheets for Retrofitting Reinforced Concrete Beams: Cracking and Tension Stiffening. *J. Reinf. Plast. Compos.* **2010**, *29*, 2647–2662. [[CrossRef](#)]
52. Pecce, M.; Ceroni, F.; Prota, A.; Manfredi, G. Response Prediction of RC Beams Externally Bonded with Steel-Reinforced Polymers. *J. Compos. Constr.* **2006**, *10*, 195–203. [[CrossRef](#)]

53. Alghazali, H.H.; Al-Jaberi, Z.K.; Aljazaeri, Z.R.; Myers, J.J. Flexural performance of Extremely Damaged Reinforced Concrete Beams after SRP Repair. In Proceedings of the 7th International Conference on Structural Engineering, Mechanics and Computation, Cape Town, South Africa, 2–4 September 2019.
54. Bencardino, F.; Condello, A. Eco-friendly external strengthening system for existing reinforced concrete beams. *Compos. Part B* **2016**, *93*, 163–173. [[CrossRef](#)]
55. Bencardino, F.; Condello, A. Innovative solution to retrofit RC members: Inhibiting-Repairing-Strengthening (IRS). *Constr. Build. Mater.* **2016**, *117*, 171–181. [[CrossRef](#)]
56. Al Nuaimi, N.; Ghous Sohail, M.; Hawileh, R.A.; Abdalla, J.A.; Douier, K. Durability of reinforced concrete beams strengthened by galvanized steel mesh-epoxy systems under harsh environmental conditions. *Compos. Struct.* **2020**, *249*, 112547. [[CrossRef](#)]
57. Katakalos, K.; Papakonstantinou, C.G. Fatigue of Reinforced Concrete Beams Strengthened with Steel-Reinforced Inorganic Polymers. *J. Compos. Constr.* **2009**, *13*, 103–112. [[CrossRef](#)]
58. Minnaugh, P.L.; Harries, K.A. Fatigue behavior of externally bonded steel fiber reinforced polymer (SFRP) for retrofit of reinforced concrete. *Mater. Struct.* **2009**, *42*, 271–278. [[CrossRef](#)]
59. Mitolidis, G.J.; Salonikios, T.N.; Kappos, A.J. Test results and strength estimation of R/C beams strengthened against flexural or shear failure by the use of SRP and CFRP. *Compos. Part B* **2012**, *43*, 1117–1129. [[CrossRef](#)]
60. Papakonstantinou, C.G.; Katakalos, K.; Manos, G.C. Reinforced Concrete T-Beams Strengthened in Shear With Steel Fiber Reinforced Polymers. In Proceedings of the 6th International Conference on FRP Composites in Civil Engineering—CICE, Rome, Italy, 13–15 June 2012.
61. Wakjira, T.G.; Ebead, U. Experimental and analytical study on strengthening of reinforced concrete T-beams in shear using steel reinforced grout (SRG). *Compos. Part B* **2019**, *177*, 107368. [[CrossRef](#)]
62. Thermou, G.E.; Papanikolaou, V.K.; Lioupis, C.; Hajirasouliha, I. Steel-Reinforced Grout (SRG) strengthening of shear-critical RC beams. *Constr. Build. Mater.* **2019**, *216*, 68–83. [[CrossRef](#)]
63. Gonzalez-Libreros, J.H.; Sneed, L.H.; D’Antino, T.; Pellegrino, C. Behavior of RC beams strengthened in shear with FRP and FRCM composites. *Eng. Struct.* **2017**, *150*, 830–842. [[CrossRef](#)]
64. Abdelrahman, K.; El-Hacha, R. Behavior of Large-Scale Concrete Columns Wrapped with CFRP and SFRP Sheets. *J. Compos. Constr.* **2012**, *16*, 430–439. [[CrossRef](#)]
65. El-Hacha, R.; Mashrik, M.A. Effect of SFRP confinement on circular and square concrete. *Eng. Struct.* **2012**, *36*, 379–393. [[CrossRef](#)]
66. Thermou, G.E.; Katakalos, K.; Manos, G. Influence of the cross section shape on the behaviour of SRG-confined prismatic concrete specimens. *Mater. Struct.* **2016**, *49*, 869–887. [[CrossRef](#)]
67. Carloni, C.; Santandrea, M.; Ravazdezh, F.; Sneed, L. Stress-strain Response of Steel-FRP Confined Concrete Columns Determined by DIC. In Proceedings of the Fourth Conference on Smart Monitoring, Assessment and Rehabilitation of Civil Structures (SMAR 2017), Zurich, Switzerland, 13–15 September 2017.
68. Thermou, G.E.; Hajirasouliha, I. Compressive behaviour of concrete columns confined with steel-reinforced grout jackets. *Compos. Part B* **2018**, *138*, 222–231. [[CrossRef](#)]
69. Thermou, G.E.; Katakalos, K.; Manos, G. Concrete confinement with steel-reinforced grout jackets. *Mater. Struct.* **2015**, *48*, 1355–1376. [[CrossRef](#)]
70. Sneed, L.H.; Ravazdezh, F.; Santandrea, M.; Imohamed, I.A.O.; Carloni, C. A study of the compressive behavior of concrete columns confined with SRP jackets using digital image analysis. *Compos. Struct.* **2017**, *179*, 195–207. [[CrossRef](#)]
71. Thermou, G.E.; Katakalos, K.; Manos, G. Experimental investigation of substandard RC columns confined with SRG jackets under compression. *Compos. Struct.* **2018**, *184*, 56–65. [[CrossRef](#)]
72. Napoli, A.; Realfonzo, R. Compressive behavior of concrete confined by SRP wraps. *Constr. Build. Mater.* **2016**, *127*, 993–1008. [[CrossRef](#)]
73. El-Hacha, R.; Abdelrahman, K. Slenderness effect of circular concrete specimens confined with SFRP sheets. *Compos. Part B* **2013**, *44*, 152–166. [[CrossRef](#)]
74. Mashrik, M.A.; El-Hacha, R.; Tran, K. Performance Evaluation of SFRP-Confined Circular Concrete Columns. In Proceedings of the 5th International Conference on FRP Composites in Civil Engineering (CICE 2010), Beijing, China, 27–29 September 2010.
75. Napoli, A.; Perri, F.; Realfonzo, R.; Ruiz Pinilla, J.G. Seismic performance of RC columns strengthened with SFRP systems: Experimental study. In Proceedings of the 10th Fiber Reinforced Polymer for Reinforced Concrete Structures (FRPRCS11), Guimaraes, Portugal, 26–28 June 2013.

76. Casadei, P.; Faella, C.; Napoli, A.; Perri, F.; Realfonzo, R.; Ruiz Pinilla, J.G. Cyclic Behaviour of RC Columns Confined with Steel Reinforced Polymer Wraps. In Proceedings of the 15th World Conference on Earthquake Engineering 2012 (15WCEE), Lisbon, Portugal, 24–28 September 2012.
77. Thermou, G.E.; Katakalos, K.; Manos, G. Influence of the Loading Rate on the Axial Compressive Behavior of Concrete Specimens Confined With SRG Jackets. In Proceedings of the ECCOMAS Thematic Conference on Computational Methods in Structural Dynamics and Earthquake Engineering (COMPDYN 2013), Kos Island, Greece, 12–14 June 2013.
78. Abdelrahman, K.; El-Hacha, R. Cost and Ductility Effectiveness of Concrete Columns Strengthened with CFRP and SFRP Sheets. *Polymers* **2014**, *6*, 1381–1402. [[CrossRef](#)]
79. De Vita, A.; Napoli, A.; Realfonzo, R. Full Scale Reinforced Concrete Beam–Column Joints Strengthened with Steel Reinforced Polymer Systems. *Front. Mater.* **2017**, *4*, 18. [[CrossRef](#)]
80. Thermou, G.E.; Pantazopoulou, S.J. Metallic fabric jackets: An innovative method for seismic retrofitting of substandard RC prismatic members. *Struct. Concr.* **2007**, *8*, 35–46. [[CrossRef](#)]
81. Valluzzi, M.R.; Valdemarca, M.; Modena, C. Behavior of Brick Masonry Vaults Strengthened by FRP Laminates. *J. Compos. Constr.* **2001**, *5*, 163–169. [[CrossRef](#)]
82. Borri, A.; Casadei, P.; Castori, G.; Hammond, J. Strengthening of brick masonry arches with externally bonded steel reinforced composites. *J. Compos. Constr.* **2009**, *13*, 468–475. [[CrossRef](#)]
83. Girardello, P.; Pappas, A.; da Porto, F.; Valluzzi, M.R. Experimental testing and numerical modelling of masonry vaults. In Proceedings of the International conference on rehabilitation and restoration of structures, Chennai, India, 13–16 February 2013.
84. Garmendia, L.; Larrinaga, P.; San-Mateos, R.; San-José, J.T. Strengthening masonry vaults with organic and inorganic composites: An experimental approach. *Mater. Des.* **2015**, *85*, 102–114. [[CrossRef](#)]
85. Carozzi, F.G.; Poggi, C.; Bertolesi, E.; Milani, G. Ancient masonry arches and vaults strengthened with TRM, SRG and FRP composites: Experimental evaluation. *Compos. Struct.* **2018**, *187*, 466–480. [[CrossRef](#)]
86. Valluzzi, M.R.; da Porto, F.; Garbin, E.; Panizza, M. Out-of-plane behaviour of infill masonry panels strengthened with composite materials. *Mater. Struct.* **2014**, *47*, 2131–2145. [[CrossRef](#)]
87. Parsekian, G.A.; El-Hacha, R.; Shrive, N.G. Strengthening and Retrofitting Unreinforced Masonry Walls with Various FRP Systems. In Proceedings of the Asia-Pacific Conference on FRP in Structures (APFIS 2007), Hong Kong, China, 12–14 December 2007; pp. 263–270.
88. Borri, A.; Castori, G.; Corradi, M. Shear behavior of masonry panels strengthened by high strength steel cords. *Constr. Build. Mater.* **2011**, *25*, 494–503. [[CrossRef](#)]
89. Borri, A.; Castori, G.; Corradi, M. Masonry Confinement Using Steel Cords. *J. Mater. Civ. Eng.* **2013**, *25*, 1910–1919. [[CrossRef](#)]
90. Sneed, L.H.; Carloni, C.; Baietti, G.; Fraioli, G. Confinement of Clay Masonry Columns with SRG. *Key Eng. Mater.* **2017**, *747*, 350–357. [[CrossRef](#)]
91. Sneed, L.H.; Carloni, C.; Fraioli, G.; Baietti, G. Confinement of Brick Masonry Columns with SRG Jackets. *Aci Spec. Publ.* **2018**, *324*, 5.1–5.10.
92. Sneed, L.H.; Baietti, G.; Fraioli, G.; Carloni, C. Compressive Behavior of Brick Masonry Columns Confined with Steel-Reinforced Grout Jackets. *J. Compos. Constr.* **2019**, *23*, 04019037. [[CrossRef](#)]
93. Jemison, S.E. Compressive Behavior of Masonry Columns Confined with Steel Reinforced Grout (SRG) Composite. Master’s Thesis, Missouri University of Science and Technology, Rolla, MO, USA, 2018.
94. Ombres, L.; Verre, S. Masonry columns strengthened with Steel Fabric Reinforced Cementitious Matrix (S-FRCM) jackets: Experimental and numerical analysis. *Measurement* **2018**, *127*, 238–245. [[CrossRef](#)]
95. Fossetti, M.; Minafò, G. Strengthening of Masonry Columns with BFRCM or with Steel Wires: An Experimental Study. *Fibers* **2016**, *4*, 15. [[CrossRef](#)]
96. Borri, A.; Corradi, M. Strengthening of timber beams with high strength steel cords. *Compos. Part B* **2011**, *42*, 1480–1491. [[CrossRef](#)]
97. Dagher, H.J.; Sanchez, O. *Hardwire Reinforced Glulam Tests*; The AEW Center Research Report; The University of Maine: Orono, ME, USA, 2005.

